American Mineralogist, Volume 70, pages 608–618, 1985

Aggregation and dissolution of small and extended defect structures in Type Ia diamond

L. A. BURSILL AND R. W. GLAISHER

School of Physics, University of Melbourne
Parkville, 3052, Victoria, Australia

Abstract

Gem quality diamonds often have up to one atom of carbon out of about one thousand replaced by nitrogen. This article reviews the structures formed by the nitrogen in various states of aggregation, ranging from a few atomic diameters up to platelet shapes several microns in extent. The understanding of such defect structures now emerging gives new impetus to studies of the geological origin and evolution of various diamond species.

Our analysis of the small defect (traditionally called point defect) structures and their mechanisms of diffusion and aggregation to form extended defects leads to the identification of essentially three stages, involving: (1) an activation energy for creation of carbon vacancies (Schottky mechanism), responsible for the production of A-centers (N–N substitutional pairs) from isolated substitutional N; (2) an activation energy for creation of split-nitrogen-interstitial/vacancy pairs (essentially a modified Frenkel defect), responsible for the conversion of A-centers into {100} platelet defects plus B-centers (nitrogen-charge-compensated vacancies) and (3) an activation energy for production of split-carbon self-interstitials (Frenkel-defect mechanism), responsible for the eventual dissolution of platelet defects and conversion of all nitrogen to an equilibrium concentration of B-centers plus nitrogen gas in void-like defects.

Introduction

Gem quality diamonds may have up to one thousand parts per million (ppm) nitrogen, forming structures ranging from a few atomic diameters up to several microns. Experimentally-induced transformations of the states of nitrogen in diamond (Evans and Zengdu, 1982) have reproduced most of the defect structures observed in natural gem-quality diamonds. In this paper, an analysis is made of aggregation and dissolution mechanisms which presumably occur during the evolution of various diamond species.

Structure of small and extended defects in diamond

Diamonds containing sufficient nitrogen to cause observable absorption in the optical spectrum between 7 and 10 μm are classified as Type I; three major subgroups are assigned, based upon the form of the absorption spectrum (Davies, 1976, 1977, 1981). In Type Ib, dispersed paramagnetic nitrogen (N center) substitutes for normal carbon sites (Fig. 1a), leaving one unsaturated bond. Type Ib is very rare in nature (0.1%) but nearly all commercial synthetic diamond is in this category. In Type IaA and IaB, nitrogen is predominantly in nonparamagnetic aggregated forms called A- and B-centers respectively (Figs. 1b, c). Type IIa and IIb diamonds are pure and transparent to UV wavelengths >220 nm; Type IIb are blue, very rare and semiconductive (due to presence of boron), whereas all other natural diamonds are electrical insulators. Type Ia diamonds, the sole concern of this paper, account for about 95% of all gem material.

Structure of small defects in diamond

Details of the important small defects are given in Table 1 and Figure 1. Note that the singly substituted carbon site (Fig. 1a), the vacancy (Fig. 1g) and the split interstitial (Fig. 1h), regarded traditionally as the obvious point defects, each contain unsaturated bonds. The split-nitrogen interstitial was not derived from spectroscopic studies, but it is the structure-building element for platelet defects in diamond. It seems that the B′ absorption (7.3 μm) in IR spectra, which has previously been correlated with platelets in diamond, may be more fundamentally due to this defect (Bursill, 1983). Both the A and B centers have been widely studied by spectroscopic methods (Davies, 1976). Nitrogen compensated defects (i.e. the A center (Fig. 1b), the B center (Fig. 1c) and the split-nitrogen-interstitial (Fig. 1i)) represent relatively stable defects, as all carbons have fully compensated tetrahedrally-directed bonds, with each nitrogen having approximately planar trigonal coordination. Note that the A center consists of a pair of nitrogen atoms substituting for carbon at adjacent sites, whereas the B center may be described as a carbon vacancy with four-next-nearest-neighbour carbons on {111} planes replaced by nitrogen in tetrahedral arrangement. Some relaxation outwards of these nitrogens gives rise to an almost perfect octahedral void (Fig. 1c).

Platelet defects. Nitrogen occurs at $\{100\}\langle\frac{1}{3}00\rangle$ platelet-shaped defects (Berger and Pennycook, 1982) from ~ 8 nm up to several μm in diameter. They have been characterized by X-ray topography, electron and cathodoluminescence

0003–004X/85/0506–0608$02.00

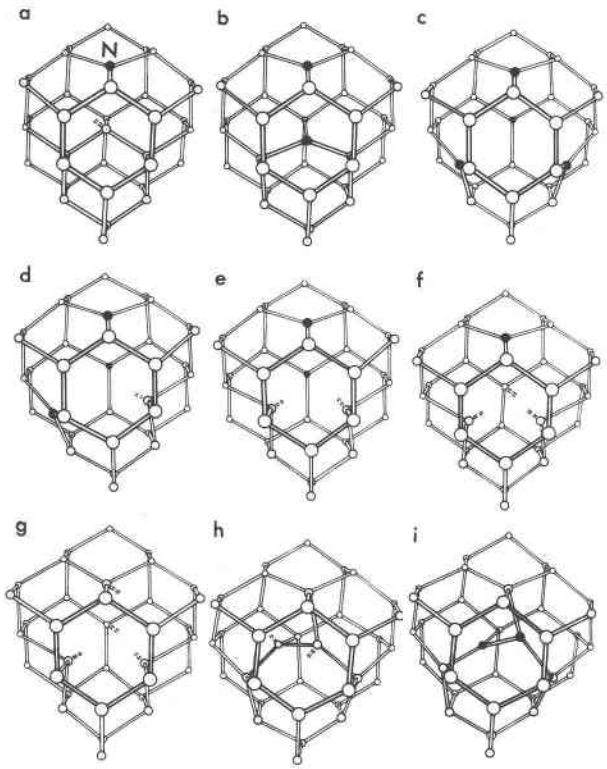

Fig. 1. Structure of small defects in diamond: (a) N center; (b) A center; (c) B center; (d) N3 center; (e) H3 center; (f) (N–V) center; (g) V center; (h) split-self-interstitial; and (i) split-nitrogen-interstitial.

Table 1. Summary of nomenclature and structure of small defects in diamond

Defect name	Description
N center	1 nitrogen replacing carbon at normal site; 1 unsaturated bond (Fig.1a)
A center	2 nitrogens substituting carbon on adjacent sites, all bonds saturated since nitrogens have triangular three-fold coordinates and carbons have tetrahedral bonding (Fig.1b)
B center	4 nitrogens substituting for carbon, forming a tetrahedron surrounding an empty carbon site; all bonds are saturated by outwards relaxation of nitrogens into triangular coordination, forming the smallest possible octahedral void (Fig.1c).
N3 center	3 nitrogens substituting for carbon, surrounding a carbon vacancy, leaving one unsaturated ("dangling") bond (Fig.1d)
H3 center	A-center trapped at vacant carbon site, giving two nitrogens surrounding a vacancy, with two dangling bonds (Fig.1e)
N-V center	1 nitrogen substituting for carbon adjacent to an empty carbon, leaving three dangling bonds
V center	Vacant carbon site, with four dangling bonds
Split-self-interstitial	2 carbon atoms replace one original site, creating two dangling bonds; note non-alignment of interstitial axis work [100]
Split-nitrogen-interstitial	2 nitrogens replace one carbon; note all bonds are saturated and interstitial axis is along [100]

microscopy (Lang, 1979) and high-resolution electron microscopy (HREM) (Barry et al., 1985), and correlate with the 7.3 μm (B') absorption. The platelet structure consists of *nonparametic* pairs of nitrogen atoms (cf. split-N-interstitial, Fig. 1i), directed along $\langle 100 \rangle$, aligned onto $\{100\}$ planes, and forming a staggered or zig-zag arrangement about a central N-only plane (see Bursill, 1983; Fig. 2); this gives an ordered half occupancy of N and C on adjacent $\{100\}$ planes. Each C has tetrahedral coordination, whereas each N has triangular coordination (Fig. 2). The interatomic parameters are consistent with known properties of C–N, C–C, C–N–C, N–C–N and C–C–N bonds (Lang, 1964), but the structure differs from Lang's model, adopting the staggered rather than the eclipsed N–N pair arrangement. Note that the zig-zag structure is anisotropic, giving differing aspects along [011] and [01$\bar{1}$], whereas the Lang model is symmetrically equivalent with respect to these directions (Fig. 2). Thus relatively low-resolution images (Lang, 1979) show highly anisotropic habits. This structure also allows small differences in C–N–C and N–C–N bond lengths and angles within the platelet, whereas the Lang model constrains these to be virtually identical with the normal C–C–C values. The up-down N–N pairs of the staggered model (Fig. 2a) produce an inversion center, whereas the eclipsed model (Fig. 2b) is quite asymmetric with respect to the diamond structure on either side of the platelet. Assuming C–C = 1.54, C–N = 1.47 and N–N = 1.44Å (Lang, 1964), there is a symmetrical mismatch of approx. −2.4% along [110] for the staggered arrangement, whereas the eclipsed model produces a highly asymmetrical mismatch of −4.8% along the one side of the platelet. Thus elasticity considerations clearly favor the staggered model. The extrinsic nature of the platelet structure (Fig. 2), with *expansion* $\langle \frac{1}{3}00 \rangle$ implies a $\{100\}$ habit plane, as $\langle 100 \rangle$ is the "softest" direction according to Young's modulus plots (Bursill and Hudson, 1978). Thus the $\{100\}$ habit minimizes elastic strain energy.

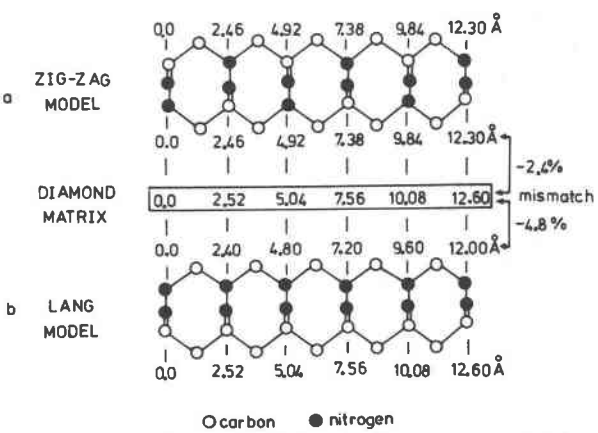

Fig. 2. Comparison of [011] projection of staggered (Barry, 1982) and eclipsed (Lang, 1964) stacking models for platelet structure. Note inversion center, with symmetrical mismatch of −2.4% relative to normal diamond for (a) and highly asymmetrical mismatch of −4.8% along one side of (b).

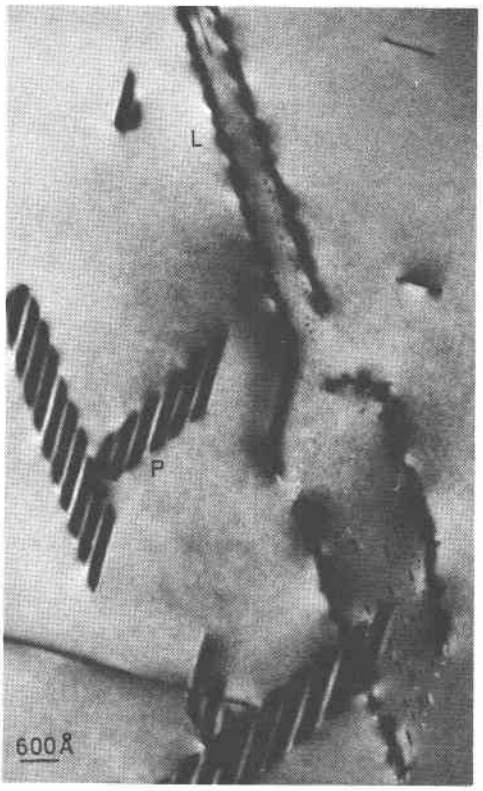

Fig. 3. Dislocation loops (L) containing small defects and also normal platelets (P): (100) platelets are seen edge-on (top left) and (010) and (001) platelets are inclined at 45° (indicated by thickness fringe contours).

Considerations of the structure of the partial dislocation terminating a platelet defect in diamond shows that [011] has considerably larger mismatching of C–N–C–N–bonds than [01$\bar{1}$], favoring the latter for the direction of preferred growth.

Void-like defects and partial platelets. In certain areas of Type Ia specimen foils, platelet defects may be large and elongated up to ~ 1 μm along one of the $\langle 110 \rangle$ directions. A small fraction ($< 5\%$) show contrast characteristics (Fig. 3) typical of perfect dislocation loops containing smaller defects (Bursill, 1983; Hutchison and Bursill, 1983). Judging from the behavior of the contrast in through-focal series of images, it seems likely that these defects are virtually voids (Anstis and Hutchison, 1982). The term voidite should not prejudice precise determination of their contents. Voidites occur within the area of the dislocation loop, and also strung along the dislocation (Fig. 5). Many of the voidites imaged seem equiaxial, ranging in diameter from 7.5–100 nm (Fig. 4). A perspective drawing of an octahedral void, aligned with [110] parallel to the electron beam (Fig. 6), shows that four of the {111} faces lie parallel to the projection axis, giving a rhomboid shape in projection. Thus the rhombic-shapes of Fig. 5 suggest regular octahedral voidites. However, elongated tubular-shaped voidites also occur (see Fig. 7) and as shown by Fig. 6, if these were aligned parallel to the projection axis in Fig. 5, they would

Table 2. Correlation between synthetic high-temperature/high-pressure treatments of diamond and the observed defect microstructures

Treatment[1]	Observed microstructures[2]
original gem[3]	N centers
2400°C, 9.5 GPa (60m)	A centers, 95% conversion, small number of N3 centers
2500°C, 9.5 GPa (2h)	B centers + platelets, and A and N3 centers
original gem[4]	A centers
2600°C, 9.5 GPa (60m) & 2700°C, 9.56 Pa (30m) & 2500°C, 9.5 GPa (180m)	A:B ratio reduced from 11.4:1 to 1.1:1

1. Data from Allen and Evans, 1978; Evans and Zengdu, 1981; Evans, Zengdu and Maguire, 1982.
2. I.R and electron microscopic techniques.
3. Original specimen Type Ib diamond containing almost exclusively singly-substituted nitrogen.
4. Original specimen Type Ia diamond containing predominantly A centers.

give identical cross-sections in projection. Thus some of the contrast variations in Fig. 5 may be due to voidites having various lengths along the projection axis.

Diffraction contrast analyses of four dislocation loops (cf. L, Fig. 3) showed the Burger's vector to be 50% prismatic and 50% shear, with extrinsic character (Woods, 1976). This implies insertion of an extra two atomic planes with respect to the surrounding diamond structure.

Structure of voidites. Construction of models of octahedral voids within the diamond structure establishes that the minimum octahedral voidite volume has 5Å triangular

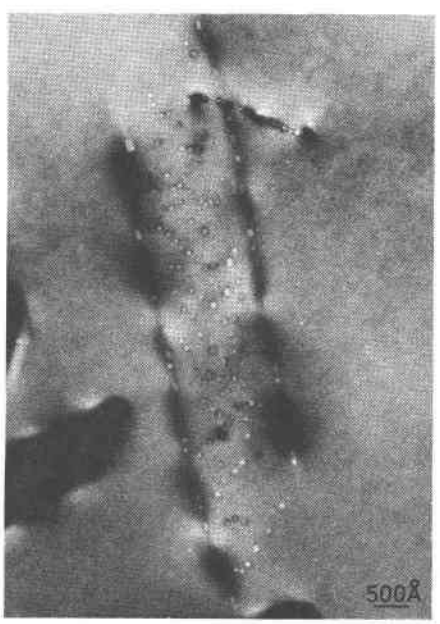

Fig. 4. Voidite contrast occurring within a dislocation loop and also along the dislocation lines of what was a (010) platelet inclined at 45° to the section.

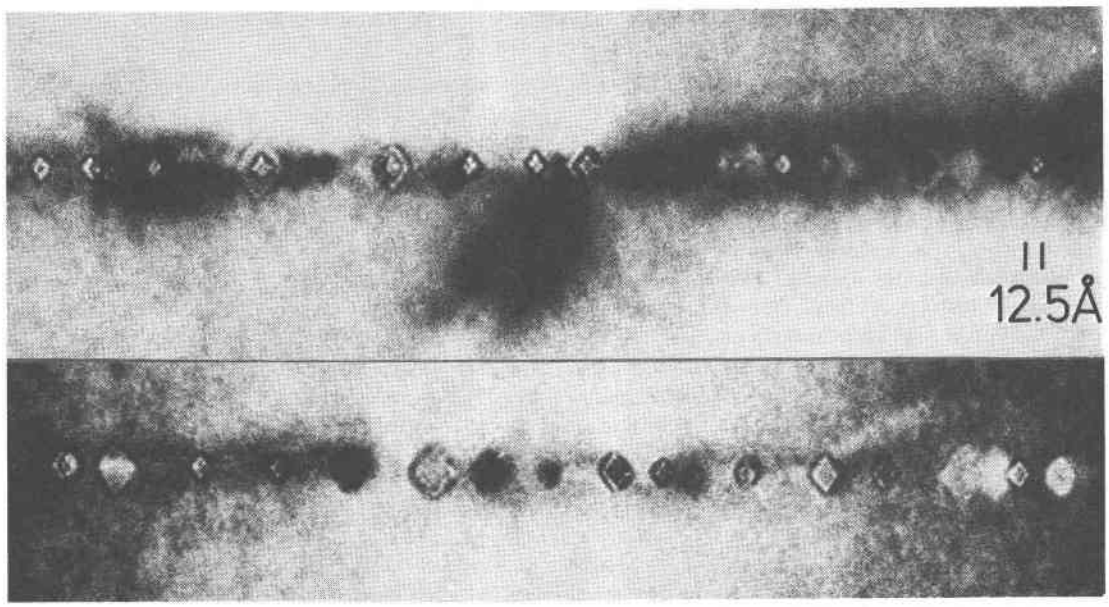

Fig. 5. Faceted voidite defects viewed along [011]. The dislocation loop lies on (100) i.e., parallel to the projection axis. Diameters range from 7.5–75Å and voidite contrast varies along the platelet.

faces. It corresponds to removal of one carbon atom and is thus a model for a single vacancy in diamond. Note, however, that this operation leaves four unsaturated bonds pointing inwards towards the vacant site. Replacing these four carbon atoms by nitrogen in three-coordination, and allowing these to relax outwards slightly, produces an almost perfect octahedral void with {111} faces. This corresponds simply to a B center (Fig. 1c). These principles extend to larger voids (see Bursill, 1983; Fig. 4 and Table 1). The ratio (R) of the number of incorporated nitrogens to the number of vacant sites is given by $R = 12n/4n^2 - 1$ where n is the "voidite order" (Barry, 1982). The voidite diameter D (line joining center of opposite faces) is given by $D = (n + 1)\, d_{111}$ where $n > 1$ and $d_{111} = 2.06$Å. Note that octahedral voids are centered alternatively at a carbon site (n odd) or at an empty 12-coordinated interstitial site (n even).

Synthetic transformations of the state of nitrogen in diamond. The various defects described above are present in widely differing proportions in different stones (Brozel et al., 1978; Davies, 1981), and gross inhomogeneities are common (Lang, 1979). These observations may be rational-

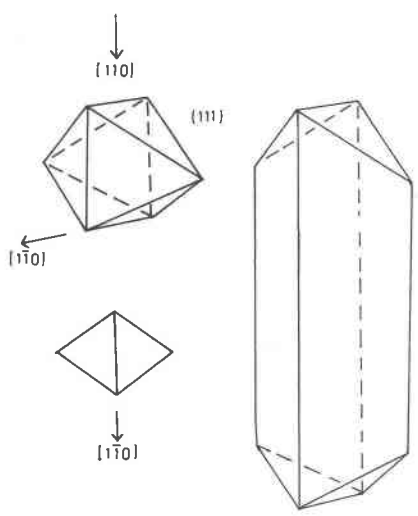

Fig. 6. Octahedral void viewed along [110], yielding rhombic-shaped projection. Elongated tubular voids (cf. Fig. 7) aligned along [110] would give identical projection.

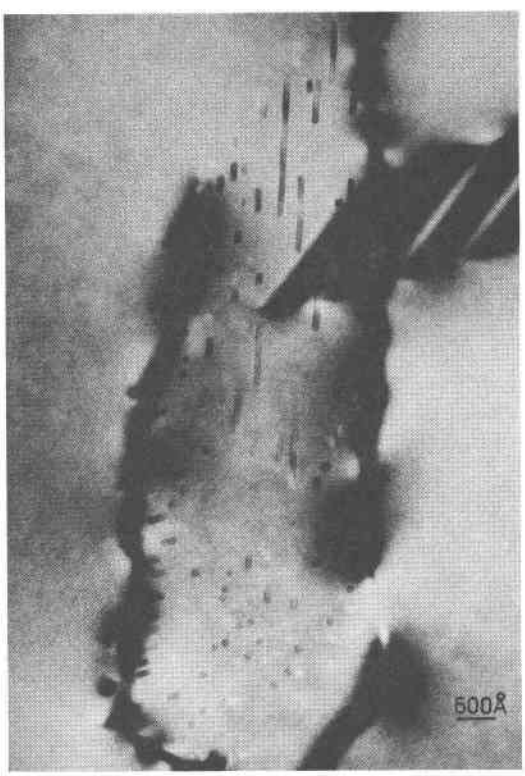

Fig. 7. Tubular voidite shapes in diamond, indicating elongation along ⟨110⟩ directions *within* the original (001) platelet defect.

ized by assuming that diamonds grew in the upper mantle of the earth, when the nitrogen was incorporated as singly substituted atoms; the nitrogen later diffused to form aggregates before the process was stopped by rapid transport to the earth's surface. Thus, most natural diamonds contain nitrogen in an aggregated form that is ESR inactive, and are thus classified as Type Ia diamonds.

All the nitrogen aggregates found in Type Ia diamonds were successfully induced in synthetic diamonds containing N-centers by heating at high temperatures under stabilizing pressures (Chrenko, et al., 1977; Brozel et al., 1978; Evans et al., 1981; Allan and Evans, 1981; Evans and Zengdu, 1982). First is the formation of A centers, which continued at 2400°C until the concentrations of A and N centers reached equilibrium. A maximum of 95% conversion was achieved, without the formation of significant numbers of B centers or platelets (Evans and Zengdu, 1982); some N3 centers were produced. Further heating to 2500°C at 9.5 GPa produced B centers and platelets, as well as A and N3 centers.

To examine the conversion of A centers to B centers and platelets, natural Type Ia diamonds were heated at 2500, 2600, and 2700°C at 9.5 GPa. The results suggest that both B centers and platelets were formed by the migration of A centers. The activation energy for conversion of A to B centers was estimated to be 6.5–7.5 eV (Evans and Zengdu, 1982).

Mechanisms for diffusion and aggregation

Stage 1: Transformation of singly substituted nitrogen into A-centers

This stage consists of dispersed N centers aggregating to form A centers (Allen and Evans, 1981; Collins, 1981), with approximately 95% conversion at 2300°C. No other centers were detected by optical absorption experiments during this first stage of aggregation.

Nitrogen migrates more readily in the presence of radiation damage (10^{22}, 2 MeV electrons/m^3; Collins, 1980), and energy calculations (Mainwood, 1981) favor a vacancy mechanism over an interstitial mechanism. The following mechanism is proposed for the aggregation of N centers into A centers (Fig. 8). Trapping of a vacancy by a substitutional N defect would produce an (N–V) center, saturating one of the original four uncompensated bonds of the vacancy. Hence the (N–V) center may be sufficiently stable to diffuse as a unit until a second N center is encountered. Two interactions are then possible; either an A center may form with the ejection of the vacancy, *or* the intermediate (N–V–N) center (H3, Fig. 1e) may be produced, further reducing the number of uncompensated bonds to two. The vacancy associated with this center could subsequently break away, leaving an A center. Both mechanisms release a vacancy which may recycle through this sequence, assuming the vacancies are not absorbed by dislocations, surfaces or interstitial defects. To account for the amount of aggregation that occurs in diamonds containing ~500 ppm N as N centers, this process must be repeated many times (Collins, 1981). The absorption line associated with the (N–V) center gradually disappears during the aggregation process (Allen and Evans, 1981), indicating a reduction in bulk vacancy concentration that limits the conversion of N centers to A centers. A simple extension of the flow diagram (Fig. 8) leads to further compensation of bonds by trapping of additional nitrogens to form N3 and B centers respectively. However, such centers were not detected at 2300°C, possibly indicating a higher activation energy for these reactions. Alternatively, the concentration of vacancies may be so low at this stage, compared with the nitrogen concentration of ~500 ppm, that insufficient N3 or B centers are formed to be detected by IR spectroscopy. At this stage, it seems the activation energy for vacancy production limits the aggregation process.

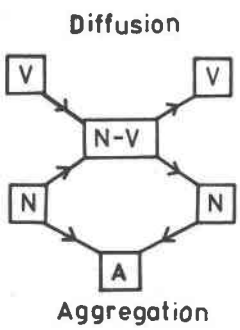

Fig. 8. Small defect interactions proposed for Stage I of nitrogen aggregation in diamond. A vacancy-diffusion mechanism allows migration of substitutional N centers. Association of N centers and vacancies allows migration of N centers. Two N centers may interact to result in an A center, releasing vacancies to recycle the process.

Stage II: Production of B centers and platelets

Further aggregation of nitrogen requires bulk diffusion of A centers. B centers *and* platelets form simultaneously in specimens heated at 2500°C (Evans et al., 1982). At the higher temperatures required for such aggregates, it might be expected that A centers would dissociate into N centers and migrate by the vacancy mechanism described above. Such dissociation is not observed, according to IR spectroscopy. Formation of B centers consumes four N atoms for each vacancy; thus for a significant number of B centers to be observed by IR spectroscopy, the vacancy concentration must reach a sizeable fraction of the N concentration (perhaps 500–1000 ppm). This implies an alternative vacancy production mechanism, with a higher activation energy than the Schottky mechanism proposed for Stage I. As platelets are also produced simultaneously with B centers in Stage II, and as these seem to consist of an ordered aggregation of N–N split interstitials (Bursill, 1983), it was suggested that the A center becomes unstable with respect to the formation of split (N–N) interstitials plus a vacancy. Further consideration shows that such a mechanism is implicit in A center migration, represented schematically in Fig. 9 and modelled in Fig. 10. Thus at the high temperatures required for Stage II aggregation (2500°C), the N atoms of the A center (Fig. 6b) create a vacant site which may subsequently dissociate from the

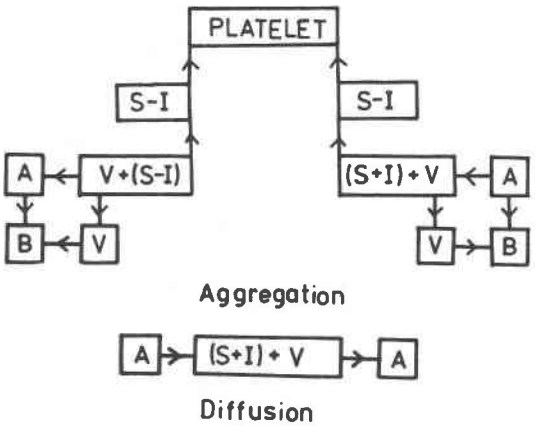

Fig. 9. Small defect interactions proposed for Stage II of nitrogen aggregation in diamond. The formation of split-nitrogen-interstitial (S-I) and vacancy (V) pairs from A centers provides a natural atomic mechanism for diffusion of A centers and leads to a relatively much higher concentration of vacancies than occurred in Stage I. Aggregation of aligned split-nitrogen-interstitials then leads to precipitation of platelet defects, whereas trapping of vacancies by A centers and to a lesser extent N centers leads to H3, N3 and B centers.

split-interstitial (Fig. 6c). Arrival of a further vacancy (at V in Fig. 6c) would then allow the split-interstitial to relax back to a symmetrically equivalent but *translated* A center (Fig. 10d, e). Repetition of this process would allow bulk diffusion of A centers. Thus split-nitrogen-interstitial/vacancy creation naturally arises during A center diffusion.

The process described so far is passive with respect to formation and/or absorption of vacancies. It closely resembles Frenkel-defect formation in perfect diamond, which produces a carbon split-self-interstitial/vacancy pair. However, given the absence of unsaturated bonds associated with the split-N-interstitial, it may have relatively lower formation energy than the split-self-interstitial, although there will be some competition between these two mechanisms, both of which provide vacant carbon sites.

If split interstitials precipitate at a platelet defect, there is an effective source of vacancies within the crystal. Trapping of A centers (or N centers) would then lead to B center formation. Again the driving force for the latter is to reduce the total number of uncompensated bonds. The net result is to simultaneously form both B centers and platelets. Note that each split-interstitial/vacancy pair formed would lead to consumption of six N centers, two going to platelets and four to B centers. An analysis of Stage II IR spectroscopic data should allow this prediction to be tested. Note that some distortion of this ratio would occur if the alternative split-self-interstitial/vacancy mechanism occurred to a significant extent. Similarly C–C interstitial pairs could also be incorporated readily into the platelet structure as a minority species, giving some variability in local stoichiometry and structure of the platelets. The presence of small numbers of such self-interstitial pairs cannot be ruled out by analysis of the HREM images. However, there are good reasons to regard self-interstitial/vacancy formation as the basis for Stage III (dissolution of platelets and formation of voidites and B centers).

During Stage II, it would seem that B centers and platelets become energetically favorable compared with A centers, as appropriate bond lengths and angles may be achieved more readily within the platelet than within either A centers or isolated split-N-interstitials, without significant long-range relaxation of the surrounding structure. The strong correlation between the B′ optical absorption at 7.3 μm and the presence of platelets, suggests that isolated split-interstitial pairs do not usually form in significant concentrations; they may occur primarily at the periphery of nucleated platelets. However, it should be noted that the optical spectra are recorded at room temperature, and not under the high-temperature/pressure conditions required for nitrogen migration and aggregation.

Platelet dissolution mechanisms and voidite formation

Giant platelets, partial platelets and voidites

Large platelets (several μm in diameter; Woods, 1976; Humble, 1982) are extrinsic with a displacement vector

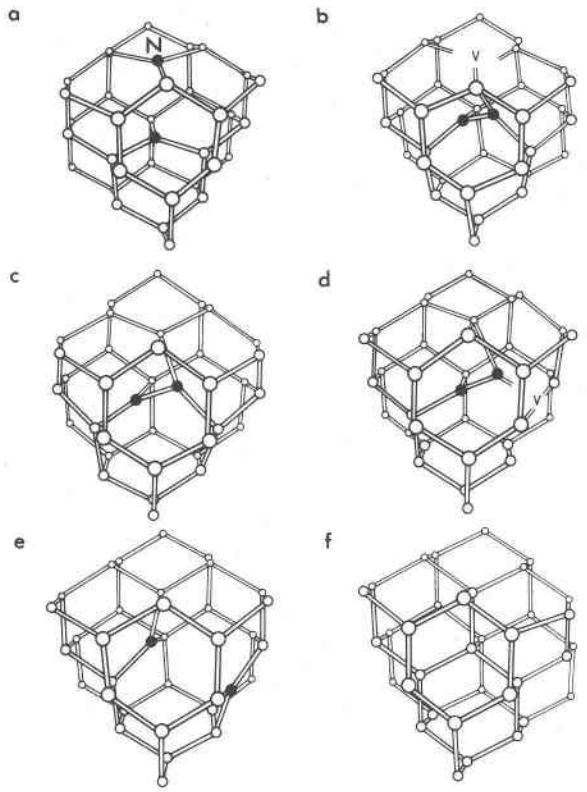

Fig. 10. Stage II agregation process in diamond: nitrogen atoms in the A center (a) move into a split-nitrogen-interstitial/configuration (b) creating a vacancy which subsequently moves away. (c) Arrival of a second vacancy (at P in d) allows the split-nitrogen-interstitial to relax back to a symmetrically equivalent but translated A center (e, f). Repitition of this process allows bulk diffusion of A centers.

approx. [0.4,0,0] (Humble, 1982). This is significantly larger than the [0.355,0,0] found for small (300Å diameter) platelets (Bursill et al., 1981). It is not clear whether this is a real difference in structure or a discrepancy between different diffraction techniques. Attempts to measure the displacement vector directly, using lattice fringes (Barry et al., 1983) have shown the severe limitations of this technique. Diffraction contrast analysis of five such loops showed them to have extrinsic nature, but the displacement vectors had 50% shear and 50% prismatic character (normal component f = 0.50) (Woods, 1976). They therefore correspond to insertion of *two* planes of (presumably) carbon atoms, replacing the *one* extra plane associated with the original platelet. Thus dissolution of a platelet requires the replacement of *two* atomic planes of nitrogen (according to the staggered model, Fig. 2a) by *three* planes of carbon. The dissolution process clearly involves the formation of voidites (Figs. 3–7) and presumably B centers. Thus it seems that at sufficiently high temperatures (higher than those achieved by Evans et al. in experiments so far), larger platelets are produced, presumably at the expense of smaller platelets but possibly also involving accretion of carbon self-split-interstitials. It seems reasonable to suggest that the onset of platelet dissolution is associated with activation of the split-self-interstitial/carbon vacancy mechanism (Stage III). This provides a ready source of both C–C interstitial pairs, which could replace the N–N pairs in the original platelet and so create the additional atomic plane required to recover the diamond structure within a perfect dislocation loop. It also provides a ready source of vacancies to be consumed in the production of B centers and voidites, thus accounting eventually for the remaining nitrogen. Several pieces of evidence favor the suggestion that the platelets are fundamentally unstable with respect to the formation of B centers at temperatures where thermodynamic equilibrium is achieved: (1) voidites appear where dislocation loops impinge; (2) a diamond which initially contained a predominance of A centers was heated to 2600° for 60 min, followed by 2700°C for 30 min, and then 2500°C for 180 min, (Evans and Zengdu, 1982); the A : B center ratio decreased from 11.4 : 1 to 1.1 : 1, with *no* obvious increase in B′ (7.3 μm) absorption; (3) plots of platelet peak absorption ($\mu_{7.3}/\mu_{7.8}^{A+B}$) versus B center absorption ($\mu_{7.8}^{B}/\mu_{7.8}^{A+B}$) show maxima for intermediate values, but zeros for both zero and maximum B center content (Brozel et al., 1978; Davies, 1981). (This last piece of evidence, from an analysis of over 50 natural stones, strongly suggests that the B center is the most stable defect in diamond.) The C–N phase diagram should show a temperature dependent solid solubility limit for N in diamond. Thus for N rich stones, the equilibrium situation may well consist of N_2 gas (perhaps trapped in voidites) plus a certain concentration of B centers. Further equilibrium studies of this phase diagram are required.

It seems that nitrogen is eventually dispersed as B centers and voidites. Platelet dissolution consumes one equivalent plane of vacant sites for every two planes of nitrogen dispersed. As each B center consumes four nitrogens and each split-interstitial carbon pair leaves one vacancy, replacement of two planes of nitrogen by three planes of carbon will leave the equivalent of one plane of vacancies, in addition to the B centers. Thus formation of voidites (containing a low nitrogen content on their surface, to compensate for otherwise unsaturated carbon bonding) would seem inevitable on dissolution of platelets and dispersal of nitrogen as B centers.

An alternative platelet dissolution mechanism, involving a pure shear Burger's vector for the dislocation loop, would require dispersal of only half of the N–N pairs, together with an equivalent plane of vacant sites, leaving half of the nitrogen within the plane of the dislocation in the form of A centers. The latter could then produce a small residual offset of the diamond structure across the (pure shear) dislocation loop. Further testing of the proposed dissolution mechanisms requires equilibration of diamonds at even higher temperatures (and confining pressures). Attempts were made to measure the total voidite volume from images for several dislocation loops (Barry, 1982), but it is difficult to be precise in the measurement of voidite volume (Fig. 6), and the smallest voids (B centers) were not imaged. The ratio (volume of voidites: volume of dispersed platelets) was 0.63, 0.47, 0.82, 0.51 and 0.79 respectively for five platelet relics, which is consistent with the above proposition that approximately one vacancy is precipitated into a voidite for each nitrogen pair dispersed. It seems likely that nucleation of platelet dissolution occurs preferentially for impinging platelets (Woods, 1976; Barry, 1982), implying high-energy local structures for direct intersection of platelets. However, it is predicted above that the *fundamental* process underlying platelet dissolution is the creation of split-self-interstitial-carbon/vacancy pairs (Stage III), which presumably has a higher activation energy than the N–N split-interstitial/vacancy mechanism required for A center migration (Stage II).

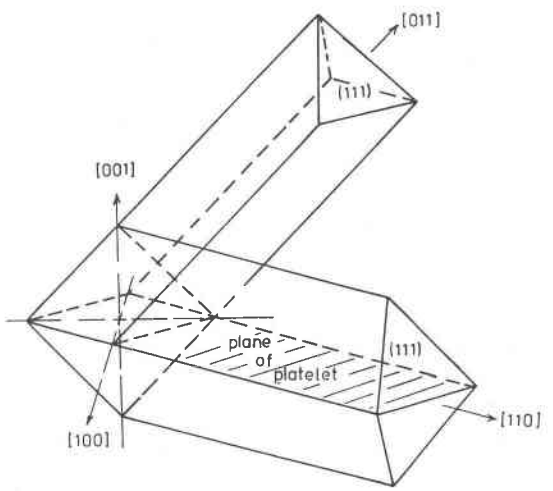

Fig. 11. Elongation of octahedral voidite along ⟨110⟩ directions, either in (i.e., [110]) or out of (i.e., [011]) the (001) plane of the original platelet defect.

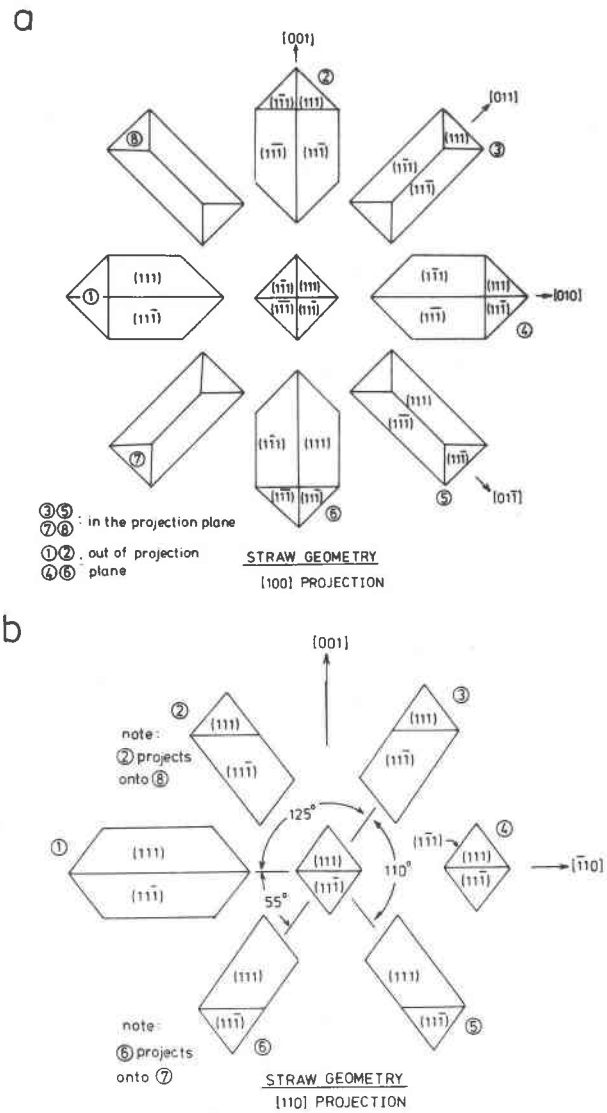

Fig. 12. [100] and [110] projections corresponding to tubular voids indicated in (Fig. 11). Tubular voids have rectangular section. Note small differences in the shapes of the terminations for tubular voids lying in and out of the (001) plane. (b) shows also the degeneracy which can occur for voidites viewed along [110] (cf. Fig. 7).

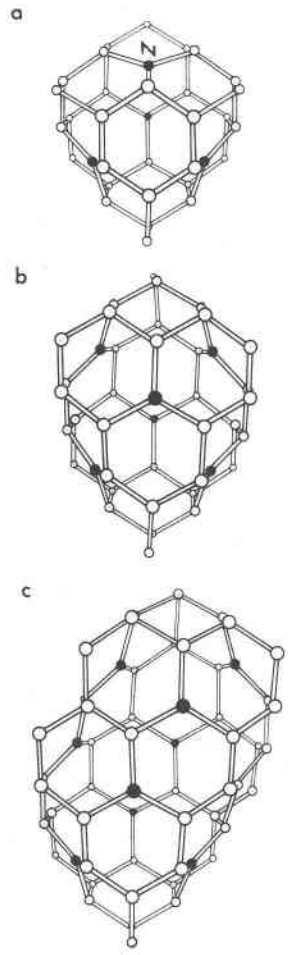

Fig. 13. Elongation of B center to produce tubular voidites; (b) is the smallest voidite having trigonal symmetry.

Voidite morphology

The rhomboid shapes of Fig. 6 indicate regular octahedral voids. However, other voidite shapes occur (Fig. 7), often being elongated up to 500Å along one of the ⟨110⟩ directions. Fig. 11 shows how an octahedral void (the minimum size would be a B center) may elongate along ⟨110⟩ directions either in or out of the (001) plane of the platelet. Note that the morphology of these voids is tubular, with rhombic cross section and {111} faceted ends (Figs. 6, 7). An important question to be answered from the experimental micrographs is whether tubular voids grow only within the {001} platelet or whether growth occurs out of the original platelet. It is not possible to determine this from one image projection, as can be seen in the corresponding [100] or [110] projections (Fig. 12a, b). For [100], all tubular voids have rectangular cross section; however, those oriented out of the plane (voids 1, 2, 4, 6)

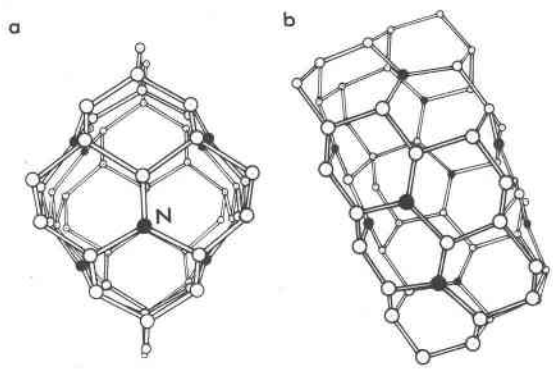

Fig. 14. [110] and [011] projections of a larger void, comparing rhombic and tubular aspects of the same void (cf. Fig. 6).

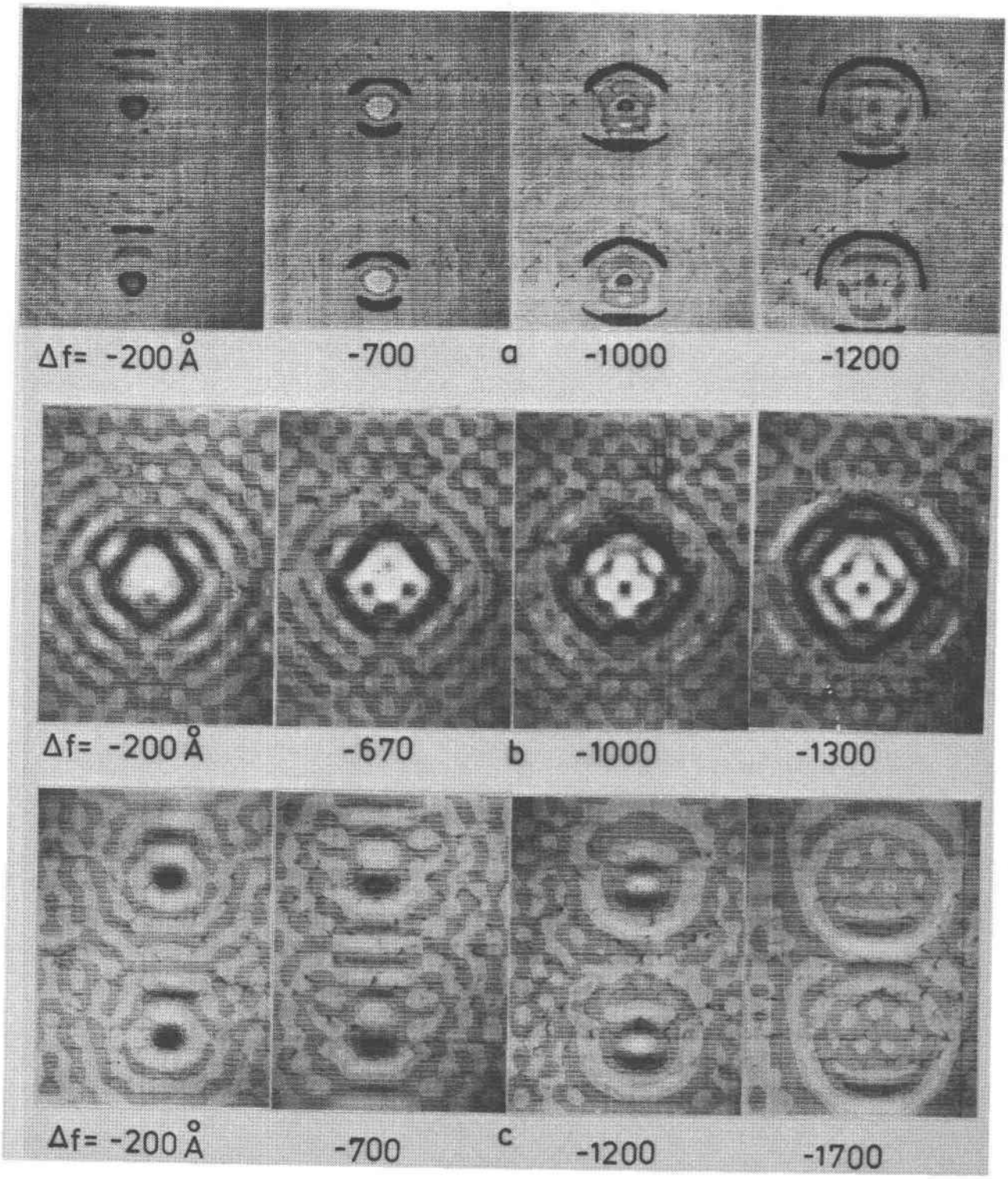
Δf= -200 Å
-700
a
-1000
-1200
Δf= -200 Å
-670
b
-1000
-1300
Δf= -200 Å
-700
c
-1200
-1700

have pointed ends whereas those lying in the plane (voids 3, 5) have 90° terminations and a small cross-section. Fig. 12b shows the degeneracy which can occur for void shapes viewed along [110]. Thus voids 3 and 5 (in the plane) have similar projections, whereas those oriented out of the plane behave as follows: (1) void 1, virtually no change; (2) voids 2, 6 develop projections degenerate with 3, 5 lying in the plane; and (3) void 4 shows rhombic ends. Despite this degeneracy, it seems unlikely that tubular voids grow out of the original platelet plane, as tubular voidites consistently show interaxial angles of 110°, never 55° or 125° (Fig. 7, 12b), and tube contrast does not appear for platelets lying parallel to the electron beam (see Figs. 3–7). Not all voidites show the same type of image contrast (see Fig. 5 for edge-on voidites), but whether the differences arise from variations of electron density within voidites, differing contribution to the image from strain diffraction contrast, or differences in faceting, may be very difficult to establish, as these three may occur in combination. A further complication arises if the voidites are in a loop lying parallel to the electron beam (cf. Fig. 5). Clearly, any of these voidites could be elongated parallel to the projection axis, when the image contrast would become a complex function of their location within the specimen foil, as well as of the usual electron optical parameters (some of these contrast effects are evident for the elongated straws in Fig. 7).

It is expected that elongation of voidites within the plane of dislocation loops or partial platelets (Figs. 6, 7) is controlled by diffusion kinetics, as vacant sites are produced at the platelet to provide a ready source of C–C split-interstitial pairs, as required for the annihilation of the original platelets. Thus vacancies, and hence voidites, are most likely to form along the partial dislocation, as it prepares to sweep further across the platelet (Fig. 4 shows voidites along dislocation lines). Such a stop-start process, where a certain concentration of vacancies (and C–C pairs) has to arise before further dissolution of nitrogen pairs can occur, leads naturally to lines of voidites—resembling tidal flow patterns—as an aftermath. Clearly the spacial and topological distribution of voidites varies widely, depending on local temperature, elastic strain and B center concentration gradients.

Voidite growth mechanisms. Tubular voidites are centered at a C–C bond center site and have trigonal symmetry. Figure 13 shows the smallest voidite. Addition of a further vacancy plus two nitrogens produces the smallest tubular symmetry void having trigonal symmetry (T center, Fig. 13). Further tubular elongation is indicated in Fig. 13c. Construction of models shows readily how voidites may change in small steps by the addition of further vacancies and A centers. Thus a B center ($n = 1$) may transform to a T, then to larger voidites having $n = 2$ etc. Figs. 14a, b show [110] and [011] projections of a larger T type center, comparing the rhombic and tubular aspects of the same void. Of course, there are many other series of possible voidite shapes and as the images show (Figs. 3–7), elongated and truncated shapes occur.

Discussion

Direct imaging of small defects and aggregates

It is natural to now ask "What is the smallest defect in the diamond structure that may be directly imaged?", "Can we image individual B centers?" Image calculations indicate that observable contrast has been obtained for voidites of order $n \geq 2$ (7.5Å diameter) (Fig. 5). Figs. 15a, b show computer-simulated images for octahedral voidites of orders $n = 1$ (B center) and $n = 2$. Such calculations allow the optimum electron optical viewing conditions to be established. Fig. 15c shows that even the split-nitrogen-interstitial may be visible if the relatively high contrast structure image is filtered out, either by careful selection of the effective instrumental resolution or by image processing. In addition, artifact contrast due to surface steps, contamination and ion or electron damage must be controlled. However, it is clear that larger aggregates, i.e., voidites of order $n \geq 2$ and platelets containing ≥ 5 split-N-interstitials, should be ready visible, even within the structure images of diamond. It now becomes important to study the nucleation and precipitation of platelet defects and the earliest stages of platelet dissolution, using HREM. For this to be useful, natural and synthetic diamonds must be treated at 2300–2700°C with confining pressures appropriate for the prevention of graphitization.

Defect structure as an indicator of thermal history. Further study of natural gem diamonds, with analyses of the type, number and statistical distribution of the different types of defects summarized in Table 2, should provide a guide to the thermal history of individual diamonds or suites of diamonds from a kimberlite pipe. This will be

Fig. 15. (A) Computed images for the [110] projection of a B center in diamond. (A spherical aberration coefficient Cs = 1.2 mm was assumed as appropriate for a 200 kV instrument). Other electron optical parameters are: crystal thickness 133Å, resolution 2.1Å, which just excludes Bragg beams, and objective lens defocus of −200Å, −700Å (near Scherzer), −1000Å, and −1200Å. Note absence of contrast features which could be used to positively distinguish the B center from other small defects (cf. Fig. 15c) or artefact contrasts. (B) Computed images for the [110] projection of voidite (order $n = 2$) in diamond. (Crystal thickness 400Å from entrance surface, resolution 2.1Å and objective lens currents of −200Å, −670Å (near Scherzer), −1000Å and −1300Å). Note the resemblance of the latter to voidite images in Fig. 3c. In general the contrast is much higher than for $n = 1$ (Fig. 15a) and shows symmetry and topology which may distinguish it from other voidite shapes and sizes, or other small defects—*provided a calibrated through-focal series of images is recorded and successfully image-matched by computer simulation.* (C) Computed images of the [110] projection of a split-nitrogen interstitial in diamond. (Crystal thickness 248Å, defect 124Å below entrance surface, resolution 2.1Å and objective lens defocus of −200Å, −700Å, −1200Å and −1700°C.) Note the lack of features which would readily distinguish it from the B center (Fig. 15a) or A center, N3 centers, etc.

useful only after sufficient synthetic work provides reliable controlled conditions for comparison with observed microstructures in natural specimens. In particular, the experiments of Evans et al. (1981, 1982) need to be extended to stage III, when platelet dissolution should occur. This will allow more controlled studies of the morphology and growth mechanisms for voidite defects. Spectroscopic studies (Davies, 1981) should be carried out concurrently with defect microstructure analyses. It would be of value to be able to determine experimentally the solubility limit of N in C as a function of temperature and pressure.

Conclusion

The structures adopted by nitrogen in Type Ia diamond have been derived by a combination of techniques. The net result seems to be that both N and C seek to achieve three- and four-coordination respectively, in the form of A and B centers, voidites or platelet defects.

Acknowledgments

The authors are grateful to Professor A. R. Lang, F.R.S., Professor T. Evans and Dr. J. L. Hutchison for their cooperation in providing specimens and in obtaining the HREM images during visits by LAB to Cambridge and Oxford in 1980 and 1981. Much of the interpretation of the platelet images was done in Melbourne by Dr. J. C. Barry. We are grateful to the University of Melbourne and the Australian Research Grants Committee for financial support, and would like to thank Dr. G. Davies and Professor T. Evans for their constructive reviews of the manuscript.

References

Allen, B. P. and Evans, T. (1981) Aggregation of nitrogen in diamond, including platelet formation. Proceedings of the Royal Society (London) A 375, 93–104.

Anstis, G. R. and Hutchison, J. L. (1982) Contrast from small octahedral voids in natural diamonds. Proceedings of 10th International Congress on Electron Microscopy (Hamburg), 2, 93–94.

Barry, J. C. (1982) Structure analysis of defects in crystals by high-resolution electron microscopy. Ph.D. Thesis, University of Melbourne, Australia.

Barry, J. C., Bursill, L. A., and Hutchison, J. L. (1985) On the structure of {100} platelet defects in Type 1a diamond. Philosophical Magazine, A51, 15–49.

Barry, J. C., Bursill, L. A., and Hutchison, J. L. (1983) Measurement of lattice displacement of {100} platelets in diamond. Philosophical Magazine, A48, 109–121.

Berger, S. D. and Pennycook, S. J. (1982) Detection of nitrogen at {100} platelets in diamond. Nature (London) 298, 635–637.

Brozel, M. R., Evans, T., and Stephenson, R. F. (1978) Partial dissociation of nitrogen aggregates in diamond by high temperature-high pressure treatments. Proceedings of the Royal Society (London) A 361, 109–127.

Bursill, L. A. and Hudson, P. R. W. (1978) High-resolution (3 Å) phase contrast studies of defects in diamond. Diamond Research 1978, De Beers Industrial Diamond Information Bureau, p. 11–16.

Bursill, L. A., Barry, J. C., Hutchison, J. L., Lang, A. R., Rackham, G. M. and Sumida, N. (1981) Voidites: a possible platelet dissociation product. Presented at Diamond Conference, Reading 1981, paper number 26.

Bursill, L. A., Hutchison, J. L., Sumida, N., and Lang, A. R. (1981) Direct measurement of lattice displacement due to platelet defects in diamond using electron microscopic Moiré patterns. Nature (London), 292, 518–520.

Bursill, L. A. (1983) Small and extended defect structures in gem-quality Type 1 diamonds. Endeavour (New Series) 7, 70–77.

Collings, A. T. (1980) Vacancy enhanced aggregation of nitrogen in diamond. Journal of Physics C: Solid State Physics 13, 2641–2650.

Collins, A. T. (1981) Diffusion and aggregation of point defects in diamond. Inst. Physics Conf. Ser. No. 59, *Defects and Radiation Effects in Semiconductors* (1980), Institute of Physics, Bristol, p. 247–252.

Chrenko, R. M., Taft, R. E., and Strong, H. M. (1977) Transformation of the state of nitrogen in diamond. Nature (London) 270, 141–144.

Davies, G. (1976) The A nitrogen aggregate in diamond: its symmetry and possible structure. Journal of Physics C: Solid State Physics 9, L537–542.

Davies, G. (1977) The optical properties of diamond. Chemistry and Physics of Carbon, 13, 1–143.

Davies, G. (1981) Decomposing the IR absorption spectra of diamonds. Nature (London) 290, 40–41.

Evans, T., Zengdu Qi, and Maguire, J. (1981) The stages of nitrogen aggregation in diamond. Journal of Physics C: Solid State Physics, 14, L379–384.

Evans, T. and Zengdu Qi (1982) The kinetics of the aggregation of nitrogen atoms in diamond. Proceedings of the Royal Society (London) A381, 159–178.

Humble, P. (1982) The structure and mechanism of formation of platelets in natural type Ia diamond. Proceedings of the Royal Society (London) A381, 65–81.

Hutchison, J. L., Bursill, L. A. and Barry, J. C. (1981) Structure of (100) platelet defects in natural diamonds. Institute Physics Conference Series No. 61. Institute of Physics, Bristol, p. 369–372.

Hutchison, J. L. and Bursill, L. A. (1983) Fresnel fringe contrast of faceted voids within gem quality diamond. Journal of Microscopy, 131, 63–66.

Lang, A. R. (1964) A proposed structure for nitrogen impurity platelets in diamond. Proceedings of the Physical Society (London), 84, 871–876.

Lang, A. R. (1979) Internal structure, Ch. 14 in "The Properties of Diamond" (J. E. Field, Ed.) Academic Press, London, p. 425–469.

Loubser, J. H. N. and van Wyk, J. A. (1978) Electron spin resonance in the study of diamond. Reports on Progress in Physics, 41, 1201–1248.

Mainwood, A. (1981) Relaxation about the vacancy in diamond. Journal of Physics C: Solid State Physics, 11, 2703–2710.

Woods, G. S. (1976) Electron microscopy of "giant" platelets on cube planes in diamond. Philosophical Magazine, 34, 993–1012.

Manuscript received, December 7, 1983;
accepted for publication, December 17, 1984.